Koen, C. (2018). Modelling the rotation period distribution of M dwarfs in the Kepler field.
Astrophysics and Space Science, 363: 11
http://dx.doi.org/10.1007/s10509-017-3225-6

Modelling the rotation period distribution of M dwarfs in the *Kepler* field

Chris Koen

Abstract

McQuillan et al. (Mon. Not. R. Astron. Soc.432:1203, 2013) presented 1570 periods P of M dwarf stars in the field of view of the *Kepler* telescope. It is expected that most of these reflect rotation periods, due to starspots. It is shown here that the data can be modelled as a mixture of four subpopulations, three of which are overlapping log-normal distributions. The fourth subpopulation has a power law distribution, with $P^{-1/2}$. It is also demonstrated that the bulk of the longer periods, representing the two major sub-populations, could be drawn from a single subpopulation, but with a period-dependent probability of observing half the true period.

1 Introduction

The primary aim of the *Kepler* mission (e.g. Borucki et al. 2010) is the detection of extrasolar planets, through the photometric signatures of their transits across the faces of their host stars. However, the well-sampled and near-continuous lightcurves of the thousands of stars in the field of view can be used for a variety of other purposes. McQuillan et al. (2013) extracted periods of M dwarfs from the *Kepler* database. Most of these periods are expected to reflect the stellar rotation periods. For an extension to higher temperature stars see McQuillan et al. (2014). Other recent relevant papers are by Hawley et al. (2014), Kado-Fong et al. (2016), Newton et al. (2016), Davenport (2017) and Rebull et al. (2017).

The aim of this paper is to rigorously model the distribution of the *Kepler* M dwarf periods P. As will be seen below, this may shed light on the number of sub-populations in this sample of cool dwarfs, as well as their individual spread in periods. This statistical summary of the data can also facilitate comparison with similar data which may be obtained in other parts of the sky.

Histograms of the periods, and their log-transforms, are plotted in Fig. 1. (Note that logarithms are to the base e: this is standard for the likelihood statistics discussed below, and using the same base throughout avoids ambiguity.) A cursory inspection shows at least three groupings: a roughly exponential distribution of periods below about 8 d; a narrow Gaussian centered on about 18 d; and a broad Gaussian with a mean in the range 30–40 d.

Since there are no periods in the range 7.44–8.42 d, the short period group is easily separated from the rest.

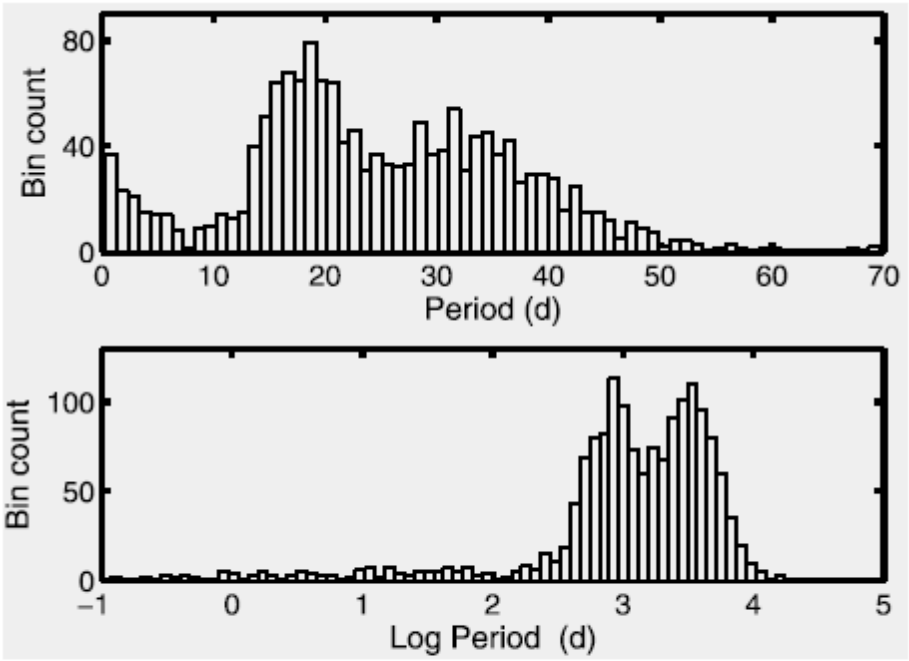

Fig. 1 Histograms of the 1570 M dwarf periods (*top panel*), and of the log-transformed data (*bottom panel*).

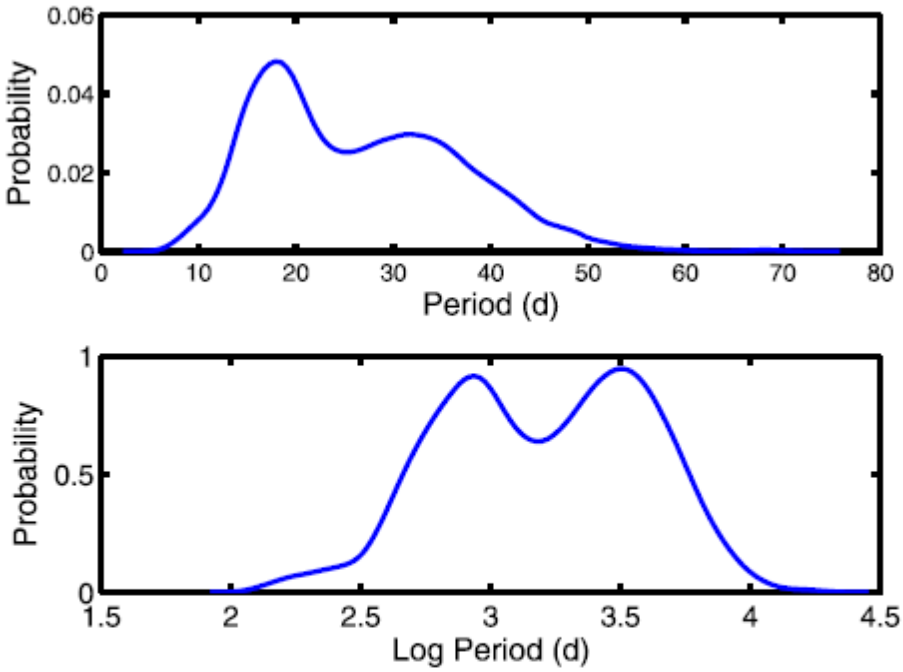

Fig. 2 Kernel density estimates of the 1437 M dwarf periods longer than 8 d (*top panel*), and of the log-transformed data (*bottom panel*). These can be thought of as smoothed versions of histograms

Sections 2 and 3 of this paper are devoted to periods longer than 8 d, while the distribution of periods below 8 d is studied in Sect. 4. Conclusions are drawn in Sect. 5.

2 Mixture modelling

If stars have two similar surface spots, separated by 180 degrees in latitude, then the measured rotation period can be half of the true period. The interested reader is referred to De Marchi et al. (2010) for a brief description: those authors refer to such rotating variables as either "R01" (single variability cycle per rotation period) or "R02" (two variability cycles per rotation period). Examination of the histogram in the top panel of Fig. 1 shows a primary peak near 18 d, with a broader secondary peak around 35 d or so. This is roughly what is expected if there is a single population of periods, roughly Gaussian, with mean near 35 d: the variance of a random subset for which $P/2$, rather than P, is measured, would be only 1/4 that of the true distribution.

McQuillan et al. (2013) showed informally that this is unlikely. Their method consisted of first separating the data into "long period" and "short period" groups, then dividing the long periods by two. If all the periods are indeed from a single population, they reasoned that this procedure should give two roughly similar distributions. However, this hypothesis was rejected by a two-sample Kolmogorov– Smirnov test.

Aside from the obvious difficulty of dividing the data into the correct groups, another potential problem with this procedure is highlighted by the Gaussian kernel density estimates of the probability density functions (PDFs) of the data, plotted in Fig. 2. The specific estimator used is robust against problems caused by multimodality—see Botev et al. (2010). Inspection reveals that the short period tails of the densities show the presence of a possible third component: this is particularly evident in the estimated PDF of the log periods. Further evidence for the reality of this component is presented below.

Given the asymmetry in the PDF in the bottom panel of Fig. 2, any powerful test statistic is bound to reject the null hypothesis tested by McQuillan et al. (2013) (on the log-periods). This problem can to some extent be circumvented by avoiding the tails of the distribution, i.e. working only with periods in the range say $14 < P < 45$ (or $2.64 < \log P < 3.81$).

A formal test can be based on fitting two competing models to the truncated distribution: the null model is

$$f_0(x) = \alpha_0 D\left(x, \mu_0', \sigma_0'\right) + (1-\alpha_0) D(x, \mu_0, \sigma_0),$$
$$L \le x \le U \qquad (1)$$

and the alternative is

$$f_1(x) = \alpha_1 D(x, \mu_1, \sigma_1) + (1-\alpha_1) D(x, \mu_2, \sigma_2)$$
$$L \le x \le U \qquad (2)$$

(In (1), the notation μ'_o and σ'_o indicates location and scale measures which are transformed version of μ_0 and σ_0. For example, if the distribution D is Gaussianon $\mu'_o = 2\mu_0$ and $\sigma'_0 = 2\sigma_0$, whereas if D is the lognormal distribution $\mu'_0 = \mu_0 + \log 2$ and $\sigma = \sigma_0$.) The PDFs in Eqs. (1) and (2) are both mixtures of two densities D. The PDF f_0 contains a fraction $1 - \alpha_0$ of periods which have been mis-identified as half the true period. In the case of f_1 no pre-specified relationship between μ_1 and μ_2 is assumed. If the probability densities D are assumed to be truncated Gaussians, defined over the interval $[L, U]$, then

$$D(x, \mu, \sigma) = \phi(x, \mu, \sigma) / \left[\Phi(U, \mu, \sigma) - \Phi(L, \mu, \sigma)\right]$$
$$\phi(x, \mu, \sigma) = \frac{1}{\sqrt{2\pi}\sigma} \exp -\frac{1}{2}\left[\frac{x-\mu}{\sigma}\right]^2 \qquad (3)$$
$$\Phi(x, \mu, \sigma) = \int_{-\infty}^{x} \phi(v, \mu, \sigma)\, dv$$

The models (1) and (2) can be fitted to the data by maximum likelihood estimation (MLE), based, as the name suggests, on maximising the log likelihood

$$\log \mathcal{L} = \sum_{j=1}^{N} \log f(P_j) \qquad (4)$$

with respect to the parameters μ_0, σ_0, α_0 (in the case of the null hypothesis) or μ_1, σ_1, μ_2, σ_2, α_1 (for the alternative hypothesis).

We follow McQuillan et al. (2013) in working with the log-transformed data: inspection of the top panel of Fig. 1 shows an extended tail to long periods, which is characteristic of a lognormal, rather then normal distribution. Fitting of (1) and (2) to truncated data with a variety of choices of lower ($13 \le L \le 15$) and upper ($42 \le U \le 46$) cut-offs reveals that (1) provides inadequate to marginal fits— the Kolmogorov–Smirnov goodness-of-fit

statistics (e.g. D'Agostino and Stephens 1986) have p-values from 2–7%. Corresponding figures for model (2) are 64–95%. It may be concluded that (1) does not, in fact, fit the data, whereas (2) does.

An alternative worth considering is that only some fraction of the "short period" group may be due to longer periods which have been mis-identified, i.e. the combination

$$f(x) = \alpha_1 D(x, \mu_1, \sigma_1) + \alpha_2 D(x, \mu_2, \sigma_2) + (1 - \alpha_1 - \alpha_2) \times D\left(x, \mu_1', \sigma_1'\right), \quad L \le x \le U \qquad (5)$$

where μ_1' and σ_1' are fully determined by μ_1 and σ_1 [see the remark following Eq. (1) above]. We pursue this in the context of modelling the distribution of all periods longer than 8 d, by fitting various mixtures of Gaussians to the (log-transformed) data. Up to three independent components are considered, with and without further *dependent* components with double periods. The results are summarised in Table 1.

Of course, the greater the number M of parameters used to model the period distribution, the better the fit and the higher the log likelihood $\log L$. Hypothesis testing can be used to compare models, compensating for this effect. Such tests are routinely based on a comparison of statistical likelihoods through the likelihood ratio statistic

$$\Lambda_* = 2(\log \mathcal{L}_1 - \log \mathcal{L}_0)$$

where L_0 and L_1 are likelihoods maximised under models 0 (the simpler) and 1 (the more complex), respectively.

Subject to certain regularity conditions likelihood ratio statistics have chi-square distributions (e.g. Andrews 2001). However, in the case of this particular problem, the regularity conditions are not satisfied—for example, some of the parameters estimated under the alternative hypothesis are not identified at all under the null. The implication is that the true distribution of the likelihood ratio is nonstandard—see the references in Miloslavsky and van der Laan (2003). McLachlan (1987) suggested establishing the distribution of the likelihood ratio statistic by Monte Carlo simulation under the null hypothesis, and this is done here.

Significance levels may then be determined as follows:

i. Fit the two models and calculate the likelihood ratio statistic Λ_*.
ii. Simulate data from the null model, using the parameter values estimated in (i).
iii. Repeat step (i), for the data simulated in step (ii), and note the value Λ_1 of the resultant likelihood ratio statistic.

iv. Repeat steps (ii)–(iii) a large number K of times, giving a collection $\Lambda_1, \Lambda_2, \ldots, \Lambda_K$ of simulated likelihood ratio statistics.

v. The significance level follows by comparing Λ_* to the collection of Λ_j generated in step (iv).

Before embarking on the exercise sketched above it is useful to look at the plot of maximised likelihoods given in Table 1, against the number of model parameters—see Fig. 3. It is clear that there are substantial gains in the likelihood as the number of parameters is increased up to $M = 8$, but that improvements thereafter are relatively small. To confirm this, we test the two hypotheses

$$H0: \quad M = 7$$
$$H1: \quad M = 8 \qquad (6)$$

and

$$H0: \quad M = 8$$
$$H1: \quad M = 9 \qquad (7)$$

The null hypothesis in (6) is rejected at a level of 0.4%. It is noteworthy that more than half of the simulated log likelihood ratios is *negative*. This may seem wrong, since the expectation is that the likelihood should always increase as the number of model parameters are increased. The reason for this peculiar result is that the null model has four modes, whereas the alternative has three: hence there are aspects of the null which cannot be reproduced by the alternative model. Nonetheless, in the case of the actual data, Λ_* is very large, implying that the alternative is far superior to the null model.

It is noted in passing that the $M = 7$ and $M = 8$ models are non-nested, i.e. neither is a special case of the other.

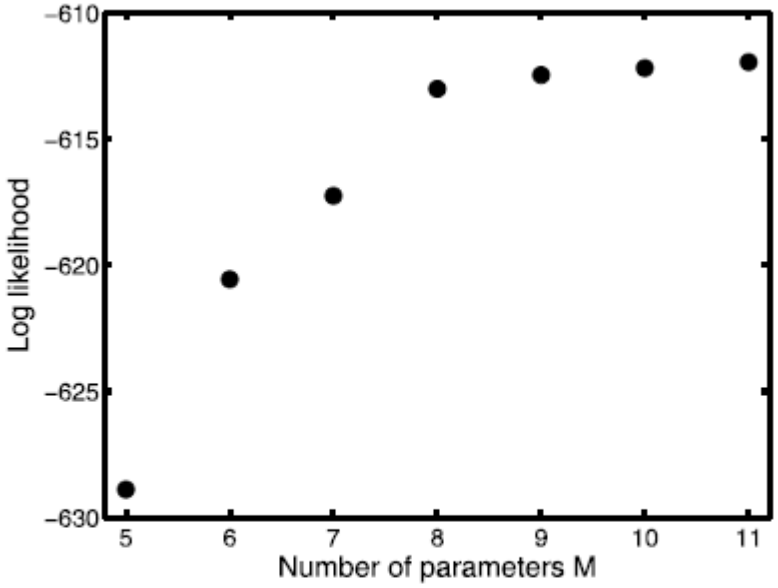

Fig. 3 Log likelihoods Eq. (4) of the models for longer periods ($P > 8$ d) in Table 1

Table 1 Details of the mixtures of normal distributions fitted to the collection of log-transformed periods longer than 8 d. Components for which means and standard deviations are indicated by primes (μ'_j and σ'_j) are not independent—see (5)

$M = 5$	$\log \mathcal{L} = -628.89$				
Means	$\mu_1 = 3.5607$	$\mu_2 = 2.9334$			
Std. Devs.	$\sigma_1 = 0.1974$	$\sigma_2 = 0.2658$			
Proportions	0.4477	0.5523			
$M = 6$	$\log \mathcal{L} = -620.56$				
Means	$\mu_1 = 2.8827$	$\mu'_1 = \mu_1 + \log 2$	$\mu_2 = 3.1233$		
Std. Devs.	$\sigma_1 = 0.1671$	$\sigma'_1 = \sigma_1$	$\sigma_2 = 0.3878$		
Proportions	0.2097	0.3125	0.4778		
$M = 7$	$\log \mathcal{L} = -617.25$				
Means	$\mu_1 = 2.2720$	$\mu'_1 = \mu_1 + \log 2$	$\mu_2 = 2.8247$	$\mu'_2 = \mu_2 + \log 2$	
Std. Devs.	$\sigma_1 = 0.1301$	$\sigma'_1 = \sigma_1$	$\sigma_2 = 0.2145$	$\sigma'_2 = \sigma_2$	
Proportions	0.0146	0.1700	0.2762	0.5392	
$M = 8$	$\log \mathcal{L} = -613.00$				
Means	$\mu_1 = 2.8973$	$\mu_2 = 2.3138$	$\mu_3 = 3.5184$		
Std. Devs.	$\sigma_1 = 0.1898$	$\sigma_2 = 0.1004$	$\sigma_3 = 0.2164$		
Proportions	0.4449	0.0231	0.5320		
$M = 9$	$\log \mathcal{L} = -612.46$				
Means	$\mu_1 = 2.3215$	$\mu'_1 = \mu_1 + \log 2$	$\mu_2 = 3.4989$	$\mu_3 = 2.8110$	
Std. Devs.	$\sigma_1 = 0.1054$	$\sigma'_1 = \sigma_1$	$\sigma_2 = 0.2261$	$\sigma_3 = 0.1525$	
Proportions	0.0257	0.1304	0.5659	0.2780	
$M = 10$	$\log \mathcal{L} = -612.17$				
Means	$\mu_1 = 2.8598$	$\mu'_1 = \mu_1 + \log 2$	$\mu_2 = 2.3057$	$\mu'_2 = \mu_2 + \log 2$	$\mu_3 = 3.4324$
Std. Devs.	$\sigma_1 = 0.1816$	$\sigma'_1 = \sigma_1$	$\sigma_2 = 0.0950$	$\sigma'_2 = \sigma_2$	$\sigma_3 = 0.2692$
Proportions	0.3570	0.2465	0.0221	0.0428	0.3316
$M = 11$	$\log \mathcal{L} = -611.94$				
Means	$\mu_1 = 3.3077$	$\mu'_1 = \mu_1 + \log 2$	$\mu_2 = 2.3054$	$\mu'_2 = \mu_2 + \log 2$	
Std. Devs.	$\sigma_1 = 0.1576$	$\sigma'_1 = \sigma_1$	$\sigma_2 = 0.0949$	$\sigma'_2 = \sigma_2$	
Proportions	0.1229	0.0066	0.0219	0.0474	
Means		$\mu_3 = 2.8723$	$\mu'_3 = \mu_3 + \log 2$		
Std. Devs.		$\sigma_3 = 0.1866$	$\sigma'_3 = \sigma_3$		
Proportions		0.3867	0.4145		

Fortunately this does not preclude use of the likelihood statistic—see e.g. the easy-to-read exposition by Lewis et al. (2011).

The null hypothesis in (7) is maintained at a level of 53%. Taken together, the results of the tests (6) and (7) therefore suggest that the eight-parameter model

$$\begin{aligned} f(\log P) = {} & 0.445\phi(\log P, 2.90, 0.19) \\ & + 0.023\phi(\log P, 2.31, 0.10) \\ & + 0.532\phi(\log P, 3.52, 0.22) \end{aligned} \qquad (8)$$

is the "best" of those entertained.

The Kolmogorov–Smirnov goodness-of-fit statistic of this model is not significant (p = 88%), showing that the fit is acceptable.

3 Proposed alternative mixture model

The means of the two dominant subgroups of periods are $\mu_1 = 34.5$ and $\mu_2 = 18.5$ d, and the respective standard deviations are $\sigma_1 = 7.6$ and $\sigma_2 = 3.5$ d. The relative fractions of periods in the two groups are $E = 0.54$ and $1 - E = 0.46$, respectively. The specific forms of some of the models in Table 1 were suggested by the closeness of μ_1/μ_2 and σ_1/σ_2 to 2, as would have been the case if there were a single population with distribution $D(\mu_1, \sigma_1)$, but the probability of measuring periods at half their true values was about 0.46. We now consider a variation on this theme, which accounts for the fact that μ_2 is slightly larger than $\mu_1/2$, namely allowing the probability of measuring the period as half the true value to *increase* with increasing period, i.e.

$$\begin{aligned} g(x) &= \left[1 - p(x)\right] f(x; \mu_1)(x) + p(2x) f(x; \mu_1/2) \\ &\equiv h_1(x) + h_2(x) \end{aligned} \tag{9}$$

where $p(x)$ (bounded by 0 and 1) is an increasing function of x.

No attempt will be made to fit the model (9) to the *Kepler* M dwarf periods; instead, it will just be demonstrated that this is a plausible explanation for the bulk of the data. Guided by the results in Sect. 2, it is assumed that the PDF f in (9) is the log-normal form. It follows that

$$\begin{aligned} h_1(x) &= \frac{1 - p(x)}{x\sqrt{2\pi}\sigma} \exp -\frac{1}{2}\left[\frac{\log x - \mu}{\sigma}\right]^2 \\ h_2(x) &= \frac{p(2x)}{x\sqrt{2\pi}\sigma} \exp -\frac{1}{2}\left[\frac{\log x - (\mu - \log 2)}{\sigma}\right]^2 \end{aligned} \tag{10}$$

For illustrative purposes the power law form

$$p(x) = \beta x^{\gamma} \tag{11}$$

is assumed.

It is required to approximate

$$\begin{aligned} f(\log P) &= \epsilon\phi(\log P, \mu_1, \sigma_1) + (1 - \epsilon)\phi(\log P, \mu_2, \sigma_2) \\ &= 0.54\phi(\log P, 3.52, 0.22) \\ &\quad + 0.46\phi(\log P, 2.90, 0.19) \end{aligned} \tag{12}$$

by (9)–(11). This is easily done by comparing moments of the two PDFs (9) and (12). Use can be made of the standard result that for x log-normally distributed with parameters μ and σ

$$\int_0^\infty x^r f(x)\,dx = \exp\left(r\mu + \frac{1}{2}r^2\sigma^2\right)$$

(e.g. Mood et al. 1974). It follows that

$$\beta \exp\left(\gamma\mu + \frac{1}{2}\gamma^2\sigma^2\right) = 1 - \epsilon$$

$$\exp\left(\mu + \frac{1}{2}\sigma^2\right) - \beta \exp\left[(\gamma+1)\mu + \frac{1}{2}(\gamma+1)^2\sigma^2\right] = \epsilon\mu_1$$

$$\beta \exp\left[(\gamma+1)\mu + \frac{1}{2}(\gamma+1)^2\sigma^2\right] = 2(1-\epsilon)\mu_2$$

$$\exp(2\mu + 2\sigma^2) - \beta \exp\left[(\gamma+2)\mu + \frac{1}{2}(\gamma+2)^2\sigma^2\right]$$

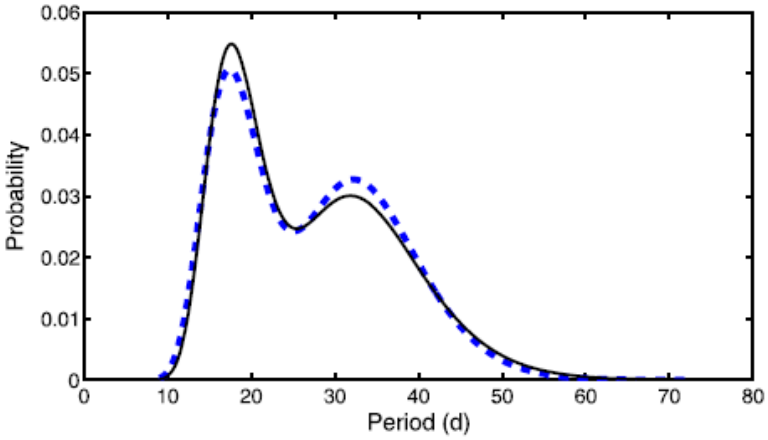

Fig. 4 A comparison between the PDF of a mixture of two independent lognormal distributions (*solid line*), and the PDF of a single lognormal distribution for which longer periods are preferentially [according to (11)] measured at half their true values (*broken line*)

$$= \epsilon\left(\mu_1^2 + \sigma_1^2\right)$$

$$\beta \exp\left[(\gamma+2)\mu + \frac{1}{2}(\gamma+2)^2\sigma^2\right] = 4(1-\epsilon)\left(\mu_2^2 + \sigma_2^2\right)$$

It is then not difficult to prove that

$$\mu = 2\log\psi_1 - \frac{1}{2}\log\psi_2$$

$$\sigma^2 = \log\psi_2 - 2\log\psi_1$$

$$\gamma = \left[\log(2\mu_2) - \log\psi_1\right]/\left[\log\psi_2 - 2\log\psi_1\right]$$

with β following from

$$\beta = (1-\epsilon)\exp -\left[\gamma\mu + \frac{1}{2}\gamma^2\sigma^2\right]$$

In these equations

$$\psi_1 = \epsilon\mu_1 + 2(1-\epsilon)\mu_2$$

$$\psi_2 = \epsilon\left(\mu_1^2 + \sigma_1^2\right) + 4(1-\epsilon)\left(\mu_2^2 + \sigma_2^2\right)$$

For the numerical values of the five parameters μ_1, μ_2, σ_1, σ_2 and E in (12) the parameters of the alternative model specified by (9)–(11) are $\mu = 3.553$, $\sigma = 0.206$, $\beta = 0.0204$ and $\gamma = 0.873$. Figure 4 compares the PDFs in (12) (solid line) and

$$f(\log P) = \left[1 - 0.0204 P^{0.873}\right] \phi(\log P, 3.553, 0.206) + 0.0374 P^{0.873} \phi(\log P, 3.553 + \log 2, 0.206)$$

(broken line). The agreement is clearly very good.

4 The short periods

The doubly-truncated power law

$$f(P) = A P^{-\alpha} = (1-\alpha) P^{-\alpha} / \left(b^{1-\alpha} - a^{1-\alpha}\right), \quad a \le P \le b \tag{13}$$

turns out to provide an excellent description of the distribution of short periods. The log likelihood function is

$$\log \mathcal{L} = n \log(1-\alpha) - n \log\left(b^{1-\alpha} - a^{1-\alpha}\right) - \alpha \sum_{i=1}^{n} \log P_i$$

For the collection of periods less than 8 d, we set a = min(P) = 0.368 d, b = max(P) = 7.438 d, and obtain the numerical solution $\hat{\alpha}$ = 0.56. An approximate standard error follows from the Fisher information as

$$\text{S.E.}(\hat{\alpha}) \approx \left(-\frac{\partial^2 \log \mathcal{L}}{\partial \alpha^2}\right)^{-1/2} = \frac{1}{\sqrt{n}} \left[b^{1-\alpha} (\log b)^2 - a^{1-\alpha} (\log a)^2 - (1-\alpha)^{-2}\right]^{-1/2} = 0.043$$

The log likelihoods for α = 0.56 and α = 0.5 are −1.8581 and −1.8592 respectively, giving a likelihood ratio statistic Λ = 0.002. According to asymptotic theory Λ should have a chi-squared distribution with one degree of freedom (Mood et al. 1974). This implies that the null hypothesis that α = 0.5 cannot be rejected, and

$$f(P) = 0.943/\sqrt{P}, \qquad 0.368 \le P \le 7.438 \tag{14}$$

is an excellent description of the 133 periods shorter than 8 d. The significance level (p-value) of the Kolmogorov– Smirnov statistic for the fit to the data of the PDF (14) is 92%.

5 Conclusions

The collection of 1570 *Kepler* M dwarf periods can be modelled as a mixture of four distributions. Three of these are overlapping log-normal distributions. There are two dominant populations (41% and 49% of all the periods) with means (standard deviations) of 18.5 and 34.5 d (3.5 and 7.6 d) (that is, before applying the logarithmic transformation). The third distribution, with mean 10.2 d and standard deviation 1.0 d, makes up only 2.1% of the total. The fourth distribution is a truncated power law with exponent statistically indistinguishable from −0.5, defined on the interval [0.37, 7.44] d. These short periods are 8.5% of the total.

McQuillan et al. (2013) present some evidence that the proper motions differ between the stars with periods in the two dominant groups. Their Fig. 12 shows a weak relation between proper motion and measured period. Scrutiny of the diagram suggests that the apparent correlation is probably primarily due to a dearth of non-zero proper motions for the longer period—and hence cooler and thus intrinsically fainter—stars. The role of selection effects is not explored, and neither is the influence of zero proper motion measurements (which appears to apply to the bulk of the stars).

Alternatively (or additionally), stars in the primary group could have a single large spot on the surface, whereas those in the secondary group have two spots separated by 180 degrees. There would only be a slight difference in the mean rotation periods: ~34.5 d for the first group, ~37 d for the second. Standard deviations would also be similar, 3.5 and 3.8 d respectively.

Section 3 presented what is, in effect, a generalisation of the eventuality investigated by McQuillan et al. (2013): there is a single population of "long" periods, with mean near 35 d. For a subsample of the stars periods are erroneously measured as half their true values, due to the fact that two minima are observed during each rotation: this happens *preferentially* for stars with longer periods. In this scenario the bimodality is essentially a consequence of two different starspot configurations.

The models summarised in the preceding two paragraphs can be combined, in the sense that the function $p(P)$ in (11) can be interpreted as a "probability" that a star has two spots, rather than one, on its surface.

It is worth noting that the methodology in Sect. 2, in particular, is general, i.e. it can be applied in any large survey to uncover potential subpopulations. There are two important caveats: the first is that mixture modelling is a mathematical exercise, designed to give a concise description of the data—there is no guarantee that different components correspond to distinct physical groupings. The second is that mixture models are not unique: it is not

uncommon to find quite distinct models which all fit the data almost equally well (see Koen and Bere 2012 for an example).

Acknowledgements The author is grateful for a South African National Research Foundation grant. Two referee's reports led to considerable clarification of the material in the paper.

References

Andrews, D.W.K.: Econometrica **69**, 683 (2001)

Borucki, W.J., et al.: Science **327**, 977 (2010)

Botev, Z.I., Grotowski, J.F., Kroese, D.P.: Ann. Stat. **38**, 2916 (2010) D'Agostino, R.B., Stephens, M.A. (eds.): Goodness-of-Fit Techniques.

Dekker, New York (1986)

Davenport, J.R.A.: Astrophys. J. **835**, 16 (2017)

De Marchi, F., Poretti, E., Montalto, M., Desidera, S., Piotto, G.: Astron. Astrophys. **509**, A17 (2010)

Hawley, S.L., Davenport, J.R.A., Kowalski, A.F., Wisniewski, J.P.,

Hebb, L., Deitrick, R., Hilton, E.J.: Astrophys. J. **797**, 121 (2014)

Kado-Fong, E., et al.: Astrophys. J. **833**, 281 (2016)

Koen, C., Bere, A.: Mon. Not. R. Astron. Soc. **420**, 405 (2012) Lewis, F., Butler, A., Gilbert, L.: Methods Ecol. Evol. **2**, 155 (2011) McLachlan, G.J.: J. R. Stat. Soc., Ser. C **36**, 318 (1987)

McQuillan, A., Aigrain, S., Mazeh, T.: Mon. Not. R. Astron. Soc. **432**, 1203 (2013)

McQuillan, A., Mazeh, T., Aigrain, S.: Astrophys. J. Suppl. Ser. **211**, 24 (2014)

Miloslavsky, M., van der Laan, M.J.: Comput. Stat. Data Anal. **41**, 413 (2003)

Mood, A.M., Graybill, F.A., Boes, D.C.: Introduction to the Theory of Statistics, 3rd edn. McGraw-Hill, Auckland (1974)

Newton, E.R., Irwin, J., Charbonneau, D., Berta-Thompson, Z.K., Dittmann, J.A., West, A.A.: Astrophys. J. **821**, 93 (2016)

Rebull, L.M., Stauffer, J.R., Hillenbrand, L.A., Cody, A.M., Bouvier, J., Soderblom, D.R., Pinsonneault, M., Hebb, L.: Astrophys. J. **839**, 92 7)